Noname manuscript No.
(will be inserted by the editor)

Predicting muscle fatigue. A response surface approximation based on proper generalized decomposition technique.

M. Sierra · J. Grasa · M. J. Muñoz · F. J. Miana-Mena* · D. González

Received: date / Accepted: date

Abstract A novel technique is proposed to predict force reduction of skeletal muscle due to fatigue under the influence of electrical stimulus parameters and muscle physiological characteristics. Twelve New Zealand white rabbits were divided in four groups ($n = 3$) to obtain the active force evolution of *in vitro Extensor Digitorum Longus* muscles for an hour of repeated contractions under different electrical stimulation patterns. Left and right muscles were tested and a total of 24 samples were used to construct a response surface based in the proper generalized decomposition. After the response surface development, one more rabbit was used to check the predictive potential of the surface. This multidimensional surface takes into account not only the decay of the maximum repeated peak force, but also the shape evolution of each contraction, muscle weight, electrical input signal and stimulation protocol. This new approach of the fatigue simulation challenge allows to predict, inside the multi-space surface generated, the muscle response considering other stimulation patterns, different tissue weight, etc.

Keywords Skeletal muscle fatigue · proper generalized decomposition · model order reduction · response surface methodology.

M. Sierra · J. Grasa · F. J. Miana-Mena · D. González
Applied Mechanics and Bioingeneering group (AMB). Aragón Institute of Engineering Research (I3A), Universidad de Zaragoza, Spain

M. J. Muñoz
Laboratorio de Genética Bioquímica (LAGENBIO). Facultad de Veterinaria. Universidad de Zaragoza, Spain

*Corresponding author: jmiana@unizar.es

1 Introduction

During a period of activity, the force output of skeletal muscle declines. This phenomena, known as fatigue, involves multitude of processes and physiological mechanisms that remain being an object of study and analysis (Bruton et al, 2000; Allen et al, 2008). One common approach used to reproduce muscle fatigue *in vitro* consists of whole muscles dissected and placed in a bath solution. The *in vitro* protocols are very popular to study skeletal muscle fatigue without nervous system interference (Aslesen et al, 2001; Clausen and Nielsen, 2007; Cairns et al, 2007, 2008; Goodman et al, 2009; van Lunteren et al, 2011; Head et al, 2011; El-Khoury et al, 2012). Moreover, it has been demonstrated that this technique, in which muscles are stimulated electrically with all fibers being activated simultaneously and repeatedly, maintains the contractile properties of the tissue regarding calcium signalling, ion exchange, oxygen diffusion and energy metabolism (de Paula Brotto et al, 2001; Thornton et al, 2011; El-Khoury et al, 2012; Park et al, 2012; Clausen, 2013a,b).

To obtain useful information in these experimental fatigue models about the rate and extent of fatigue, there have been several attempts to curve-fit the entire fatigue profile (*i.e.,* peak maximum force/stress *vs* time). For a review of different aproximations in this context, the reader is referred to the work of Cairns et al (2008). Although these fittings ensure quantitative comparisons of fatigue with different stimulation protocols, they involve averaging curves and interindividual differences are neglected (Cairns et al, 2008). Moreover, the information contained in the force development of individual contractions is not considered.

The response surface methodology (RS) has been used successfully in many research works in the biome-

chanics field in optimization studies (Lin et al, 2006; Nirmalanandhan et al, 2008; Eberle et al, 2013), experimental (Zhao et al, 2012) and computational test design (Sigal and Whyne, 2010), looking for critical variables in a complex problem (Wang et al, 2005), etc. Basically, response surfaces are multidimensional surfaces fit to quantities of interest which mathematical form allows easy interpolations to obtain another realization with a different combination of parameters. The multidimensional approximation increases its complexity and computational cost due to the well-known "*curse of dimensionality*" (Ladeveze and Chamoin, 2011). To reduce this order of complexity, the use of the response surface methodology combined with the technology of model reduction, known as proper generalized decomposition (PGD) (El Halabi et al, 2013b), is proposed in this work. This latter technique, based on the use of separated representations, was developed for solving multidimensional models (Ammar et al, 2006, 2007) and in the context of stochastic modeling (Nouy, 2007). The technique was extended for addressing parametric models, where model parameters were considered as model extra-coordinates. This made possible the calculation of the parametric solution that can be viewed as a metamodel or a computational vademecum, to be used for real-time simulation, optimization, inverse analysis and simulation-based control (Chinesta et al, 2013).

The study reported here was conducted with the main objective of investigate the potential of the RS with the technology of PGD to predict the fatigue response of skeletal muscle. In this way, a multidimensional surface was fitted to a limited number of experimental results obtained in an *in vitro* animal model. Afterwards, in order to validate our model, a new *in vitro* experiment was carried out using a different parameter combination from those used to develop the model. The results obtained were compared with the response prediction given by our model.

The paper is established as follows: In the next section the animal model and stimulation protocols to obtain the experimental data are presented. Then, a brief description of RSPGD for a general multidimensional case is presented and several numerical examples are introduced. Finally, the possibilities of the method, its cost and accuracy for different design parameters are discussed and different concluding remarks presented.

2 Material and Methods

The experimental study was conducted on thirteen male New Zealand White rabbits aged two months and with a body mass of 2150 ± 50 g. All experiments were approved by the University of Zaragoza Ethics Committee for the use of animals in experimentation in accordance with the provisions of the European Council (ETS 123) and the European Union (Council Directive 86/609/EEC) regarding the protection of the animals used for experimental purposes. The animals were kept in a temperature controlled room ($22 \pm 1\,^{\circ}$C) with 12h light-dark cycles and free access to water and food.

2.1 Muscle preparation

Animals were anesthetized with a Medetomidine (0.14 mg/Kg), Buprenorfine (0.02 mg/Kg) and Ketamine (20 mg/Kg) protocol and then euthanized by an intravenous overdose of sodium pentobarbital. Immediately afterwards, the animal was placed on its back and a midline incision was done to the ankle in the midsection of the knee. *Tibialis Anterior* (TA) was removed to access to the *Extensor Digitorum Longus* (EDL). The EDL muscle was carefully extracted by cutting off the distal and proximal tendons. Then, a cyanoacrylate sandpaper tab was pasted to both tendons in order to ensure a perfect attachment to the machine.

2.2 Protocol stimulation

Functional *in vitro* testing of rabbit muscles were carried out in a methacrylate organ bath ($20 \times 20 \times 20$ cm) designed by the authors to be installed in an electromechanical Instron Microtester 5248. The distal tendon of each muscle was strongly fixed inside the bath and the proximal tendon of the muscles samples were also fixed to the machine actuator with a 50 N full scale load cell (Fig. 1.a). Once the sample is vertically fixed, the temperature of the oxygenated Ringer's solution was maintained pumping it through a separate temperature controller and back to the organ bath. This physiological environment ($27\,^{\circ}$C and oxygen saturated solution) assured a physiological response to the electrical stimulation. To this aim, a pair of platinum plate electrodes running the length of the isolated muscle on either side were connected to a CIBERTEC CS-20 electrical signal generator. The gap between these plates can be regulated to avoid the contact with the tissue. Thus, the muscle was stimulated by the electrical field generated by the electrodes and not by direct contact (see Fig. 1.a). Before the fatigue protocol, each sample was subjected to a length sweep with short active stimulation in order to determine its optimal length.

Twelve rabbits were divided in four groups (3 animals per group), in each group left and right EDL were tested ($n = 6$). The amplitude of the electrical impulse was fixed to 100 V for all the groups as well as the

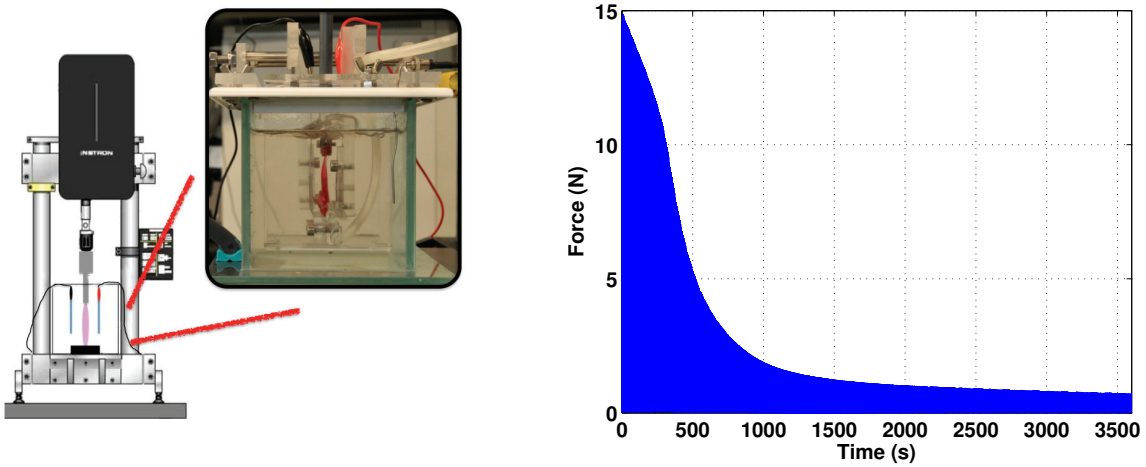

Fig. 1 (a) Scheme of the experimental setup using an universal testing machine. (b) Raw data for evolution of muscle force registered by the data acquisition software.

Table 1 Electrical stimulation parameters selected for the different groups. The amplitude of the signal was fixed at 100 V.

	Pulse duration (s)	Frequency (Hz)	Stimulation time (s)	Rest time (s)
Group 1	–	–	0.2	6
Group 2	0.001	40	0.2	10
Group 3	0.001	60	0.2	10
Group 4	0.001	100	0.2	10

stimulation time, fixed to 0.2 s. In the first group, EDL muscles were stimulated with a continuous signal with 100 V amplitude . The interval between train of pulses was 6 s. All the other groups received the same pulse duration (1 ms) and the same rest time (10 s). However, the frequency was 40 Hz for the second group, 60 Hz the third group and 100 Hz the fourth one. All the muscles were stimulated for one hour. The different parameters for each group are presented in Table 1.

Finally, after the development of the response surface and in order to validate its predictive potential, one more rabbit was used. The signal applied to the right EDL sample consisted of 0.005 s pulses at 80 Hz during 0.2 s. The amplitud of the signal was maintained at 100 V and the time interval between train of pulses was fixed to 10 s.

In Fig. 1.b the raw data obtained for one sample during the one hour protocol can be observed. The acquisition software recorded force and time pair of values when the force developed by the tissue increased or decreased 1 mN.

2.3 The RSPGD approach

In this section a brief description of the Response Surface using Proper Generalized Decomposition methodology (RSPGD) (El Halabi et al, 2013b) is presented.

The RS can be easily explained as the best approximation response function $f(x_1, x_2, \cdots, x_n)$ partially defined by a cloud of values of that function coming from external numerical results, experiments, or any other source of data. This response function dependent on the values of n input variables or quantitative factors $\mathbf{x} = \{x_1, x_2, \cdots, x_n\}$ which are considered capable of define a hyper surface in the bounded region $\Omega \subset \mathbb{R}^n$ (called the experimental region) in which we consider constrained the values of $\mathbf{x}$ by practical limitations.

Many types of functions have been used as approximation functions determining their associated constants using a regression analysis, like least squares technique. Other fitting methods, such as weighted least squares regression, best linear unbiased predictor used for Kriging, back-propagation mostly implemented in neural networks, and many others (Nakashima, 1995; Sakata et al, 2007; Arellano-Garcia et al, 2007; Park and Park, 2010; Koutsourelakis, 2008; Langley and Simon, 1995), can be used for this proposal.

However, the fitting procedure for high-dimensional spaces is not frequently found and has not been implemented due to its intrinsic complexities (Lesh, 1959). The use of high number of parameters to handle for a high-dimensional fitting increases exponentially with the number of dimensions. To avoid the so-called "*curse of dimensionality*" that appears in traditional strategies, model reduction techniques has been developed in the last years. The main characteristic of model reduction methods are that the response of complex models

can be approximated by the one of a surrogate model which represents the projection of the initial model on a low dimensional reduced basis (Nouy, 2010). The difference between the different model order techniques is the way of defining and constructing this basis. The RSPGD methodology applied in this work, uses a model reduction method based on separation of variables called Proper Generalized Decomposition (PGD) (Ammar et al, 2006, 2007; Chinesta et al, 2010b; Gonzalez et al, 2010). PGD have been introduced in different contexts like parameterized PDEs (Nouy et al, 2008; Nouy, 2009; Nouy and Le Maitre, 2009; Doostan and Iaccarino, 2009), multi-scale models (Chinesta et al, 2010a; Neron and Ladeveze, 2010; El Halabi et al, 2013a), parametric modeling and structural optimization (Leygue and Verron, 2010), multi-dimensional PDEs (Ammar et al, 2006, 2007; Gonzalez et al, 2010; Nouy, 2010), non-linear models (Niroomandi et al, 2013a,b), dynamic behavior (Gonzalez et al, 2014), etc.

This technique is a greedy algorithm that constructs the approximation of the solution by means of a sum of products (sometimes called finite sum decomposition) of separated one-dimensional functions depending on each of the problem dimensions or parameters. Each of these functions is determined by an iterative method, with no initial assumption on their form, although usually, they are expressed as piecewise linear splines with small support as in standard linear one-dimensional finite elements.

Let $\psi(\mathbf{x})$ be a scalar function of $\mathbf{x} = (x_1, x_2, \cdots, x_n) \in \Omega = \prod_{i=1}^{n}[l_i, L_i]$. In the PGD approach, this function is approximated as:

$$\psi(\mathbf{x}) \approx \sum_{i=1}^{T} \omega_i \prod_{k=1}^{n} F_i^k(x_k) = \sum_{i=1}^{T} \omega_i F_i \tag{1}$$

with $F_i^k(x_k)$ the $i-th$ one-dimensional function of the $k-th$ variable x_k that has to be computed in an implicit scheme, n the number of independent variables (dimensions), F_i the product of n functions F_i^k and T the number of sums or terms for the approximation.

For the fitting procedure in each dimension, a least square approach is established. Given a set of pairs $(\mathbf{x}_m, \psi_m)$ with $m = 1, \ldots, D$ known values of the function ψ for D combinations of independent parameters, find the function $F(\mathbf{x})$ expressed as in (1) which minimizes E defined as:

$$E = \sum_{m=1}^{D} [\psi_m - F(\mathbf{x}_m)]^2 \tag{2}$$

Where, $F_i^k(\mathbf{x}_k)$ are usually expressed in discrete form as:

$$F_i^k(\mathbf{x}_k) = \sum_{j=1}^{J_k} N_j^k(\mathbf{x}_k) z_{ij}^k \tag{3}$$

with N_j^k the standard linear one-dimensional shape function evaluated in $\mathbf{x}_k$, z_{ij}^k the nodal value vector of the function F_i^k at node j. For minimization of E, the partial derivatives with respect to the parameters of $F(\mathbf{x})$ must be zero. The algorithm consists in an iterative procedure to add new terms in the finite sum until convergence of the solution. To this end, a three steps are proposed:

1. **Projection Step** Compute the coefficients ω_i from the linear system of equations derived from the minimization of the functional E with respect to the coefficients ω_i

$$\frac{\partial E}{\partial \omega_i} = 2 \sum_{m=1}^{D} [\psi_m - F(\mathbf{x}_m)] \frac{\partial F}{\partial \omega_i} \ , \qquad i = 1, \ldots, T \ ; \tag{4}$$

The equivalent linear system may be expressed as:

$$\mathbf{K}\omega = \mathbf{f} \tag{5}$$

2. **Convergence Step** A convergence check for the overall solution is proposed in this stage, that is, for the already computed values of the basis functions $F_i^k(x_k),\ i = 1, \ldots, T\ ;\ k = 1, \ldots, n$ and coefficients $\omega_i,\ i = 1, \ldots, T$ the value of the relative error ϵ must be below a certain predefined accuracy limit.

$$\epsilon = \sqrt{\frac{E}{\sum_{m=1}^{D}[\psi_m]^2}} < \text{TOL} \tag{6}$$

with E given by (2).
If this condition is fulfilled the solving process finishes and if not, we move to the next step.

3. **Enrichment Step** A new term $T+1$ is added to the finite sum, so the new basis functions $F_{T+1}^k(x_k),\ k = 1, \ldots, n$ have to be obtained. In this "enrichment stage" (Ammar et al, 2006; Gonzalez et al, 2010) the response function is then written as:

$$F(x_1, \ldots, x_n) = \sum_{i=1}^{T} \omega_i \prod_{k=1}^{n} F_i^k(x_k) + \prod_{k=1}^{n} R^k(x_k) \tag{7}$$

Here $F_{T+1}^k(x_k)$ has been substituted by $R^k(x_k)$ since the normalized basis functions $F_{T+1}^k(x_k)$ will be obtained by normalizing the functions $R^k(x_k)$ once the iterative process described below converges. To compute the enrichment functions, a non-linear problem

Table 2 Intervals and discretization of each parameter for the EDL

Factor	Initial Value	Final Value	Number of Elements
Frequency (Hz)	35	110	1
Pulse duration (s)	0.0001	0.015	1
Muscle weight (g)	1.2	2.75	2
Animal weight (kg)	1.1	2.9	2
Rest time (s)	5	11	1
Total time (s)	0	3600	100

with as many equations as the number of dimensions ($k = 1, 2, \cdots, n$) and obtained by replacing (6) into (2), must be solved.

The intervals and discretization of the variables considered in the response surface are presented in Table 2.

3 Results

3.1 Experimental results

Average muscle weight, length and volume together with standard deviation are presented in Table 3. In order to obtain an estimation of the cross sectional area (CSA) of the muscles, the technique proposed by Calvo et al (2010) was followed, results are shown in Table 4.

Table 3 Muscle weighs, muscle lengths and muscle volumes from each experimental group recorded by the authors.

	Muscle weight $\pm SD$ (g)	Muscle length $\pm SD$ (mm)	Muscle volume $\pm SD$ (ml)
Group 1	2.34 ± 82.94	68.4 ± 0.54	2.32 ± 0.1
Group 2	2.42 ± 69.46	60.25 ± 1.5	2.37 ± 0.05
Group 3	2.07 ± 226.18	57.25 ± 4.99	2.02 ± 0.28
Group 4	2.10 ± 128.04	60.25 ± 4.42	2.07 ± 0.15

All the muscles were at optimal length before starting experiments in order to obtain maximal force production. Length sweep registration can be observed in Fig. 2.

Table 4 Cross Sectional Area estimated from muscle measurements.

	CSA $\pm SD$ (mm^2)
Group 1	33.64 ± 1.20
Group 2	39.55 ± 0.6
Group 3	35.50 ± 1.6
Group 4	34.43 ± 2.73

In Fig. 3 the experimental results are presented in the classical form in which the peak maximum stress evolution is averaged for the samples in the four groups. There were no significant differences among groups. Nevertheless, the Group 1 experimented the greatest decline, showing at $t = 1000$ s a reduction of around a 87.5%.

Fig. 4.a represents the evolution of the normalized force for the different contractions along the fatigue protocol for one of the samples (Group 1). In the figure, only every ten pulses are shown to allow a correct visualization. This evolution can be represented in a 3D plot where the third axis is the number of pulses or contractions. Plotting every ten pulses the result can be observed in Fig. 4.b. Analyzing the evolution of the pulses only the first seventy are monotonically increasing until the impulse ends. From that point, the pulses experimented increasing sag until the 100-th pulse approximately and then the sag remained more or less constant.

3.2 RSPGD approximation results

The experimental data were obtained using the protocol defined in Section 2 and a total of 12 samples were considered. The solution obtained using the RSPGD algorithm were the vectors that represent the basis functions of the approximation and its respective ω values, with which it is possible to evaluate the response at any point of the multi-dimensional domain.

In order to check the behavior of the response surface to obtain new values for the muscle forces, a numerical test has been developed. The response surface was evaluated at the same stimulation parameters selected for the last sample described in Section 2. The evolution of the maximum peak force for the computational and experimental results can be observed in Fig. 5.a. A comparison between the 50-th contraction is represented in Fig. 5.b. The computed relative error between the RS prediction and the experimental result is less than 13%. Finally, the evolution of all the contractions are shown in 5.c.

4 Discussion and Conclusions

Experimental EDL force registered through the one hour stimulation, showed a characteristic profile corresponding with fast-twitch muscles, where a significative drop of 80% of initial force is usually observed after 1000 s of stimulation. Similar force decline was characterized

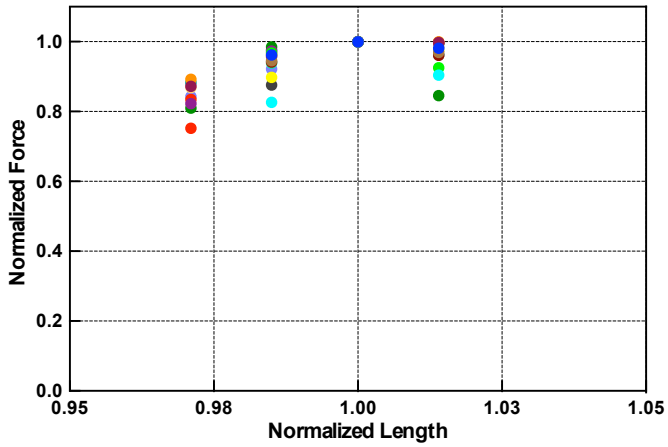

Fig. 2 Relationship obtained for all the muscles tested. Optimal muscle lengths were fixed to register maximum forces.

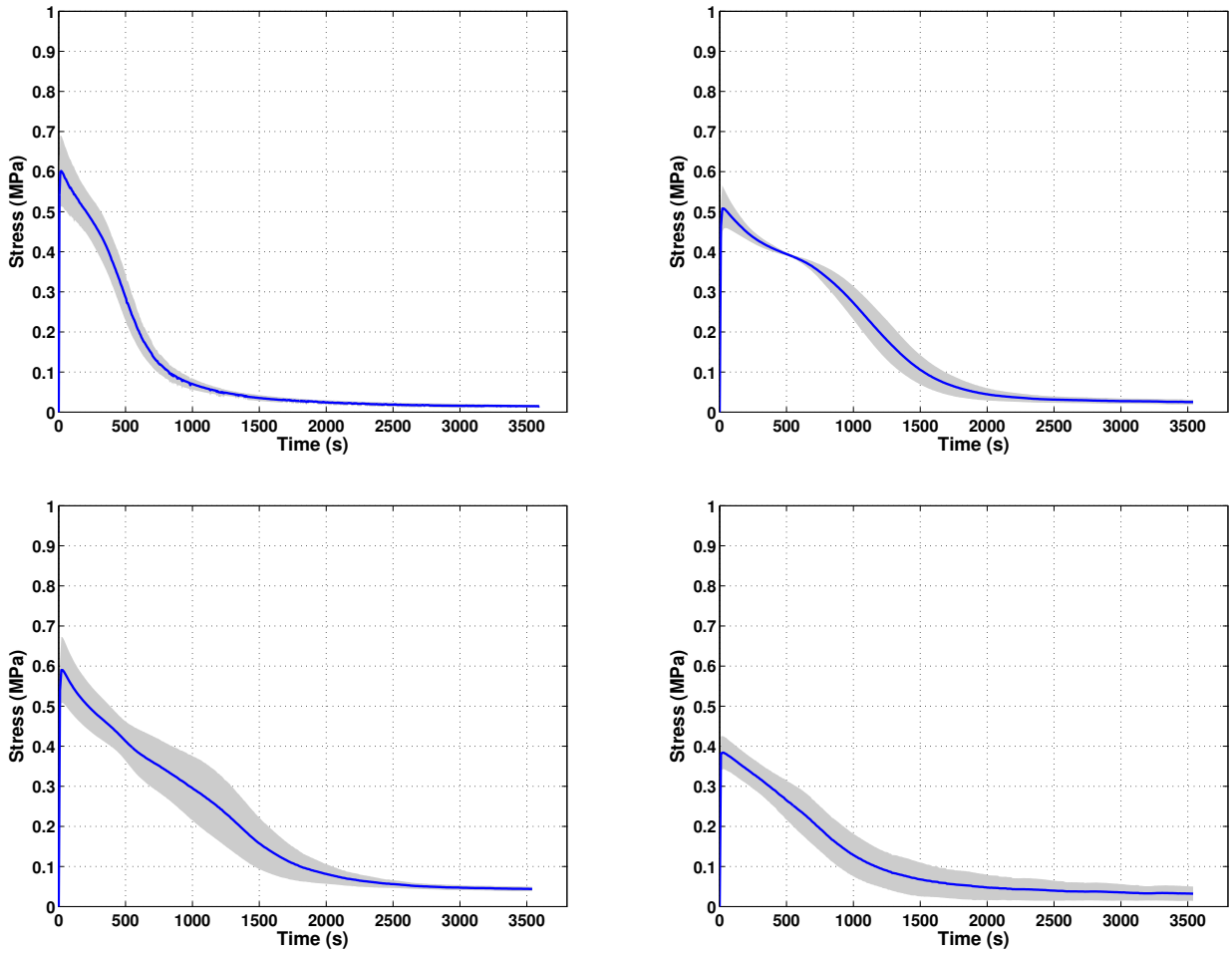

Fig. 3 Evolution of maximum stress developed by EDL muscles under the different stimulation protocols presented in Table 1. The amplitude of the signal was the same for all groups (100 V). The continuos line represents the average peak maximum value and the grey regions are the ± standard deviation bounds.

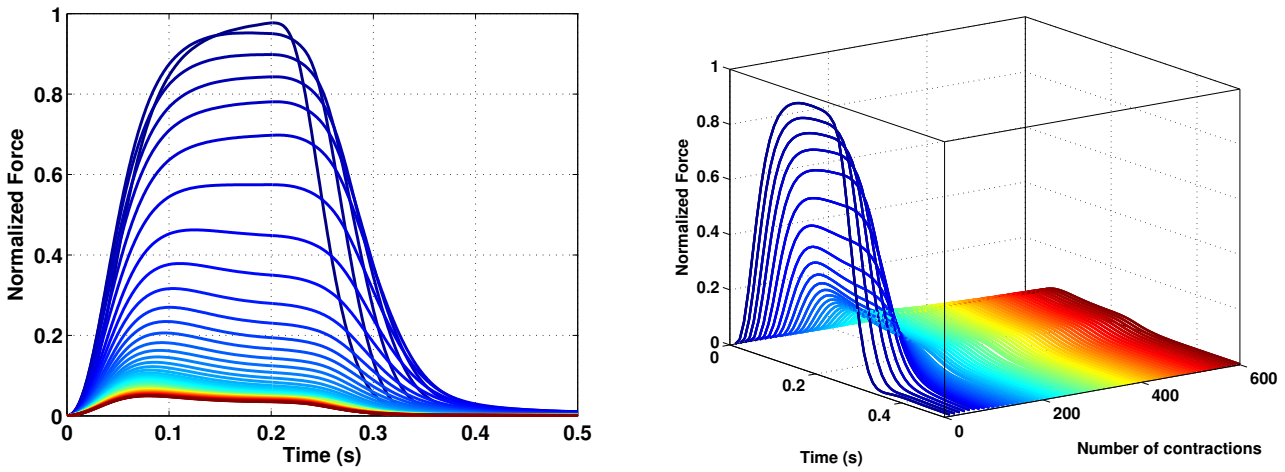

Fig. 4 Experimental data: a) Evolution of EDL force and its contraction shape through time b) Contraction evolution of EDL in a 3D representation.

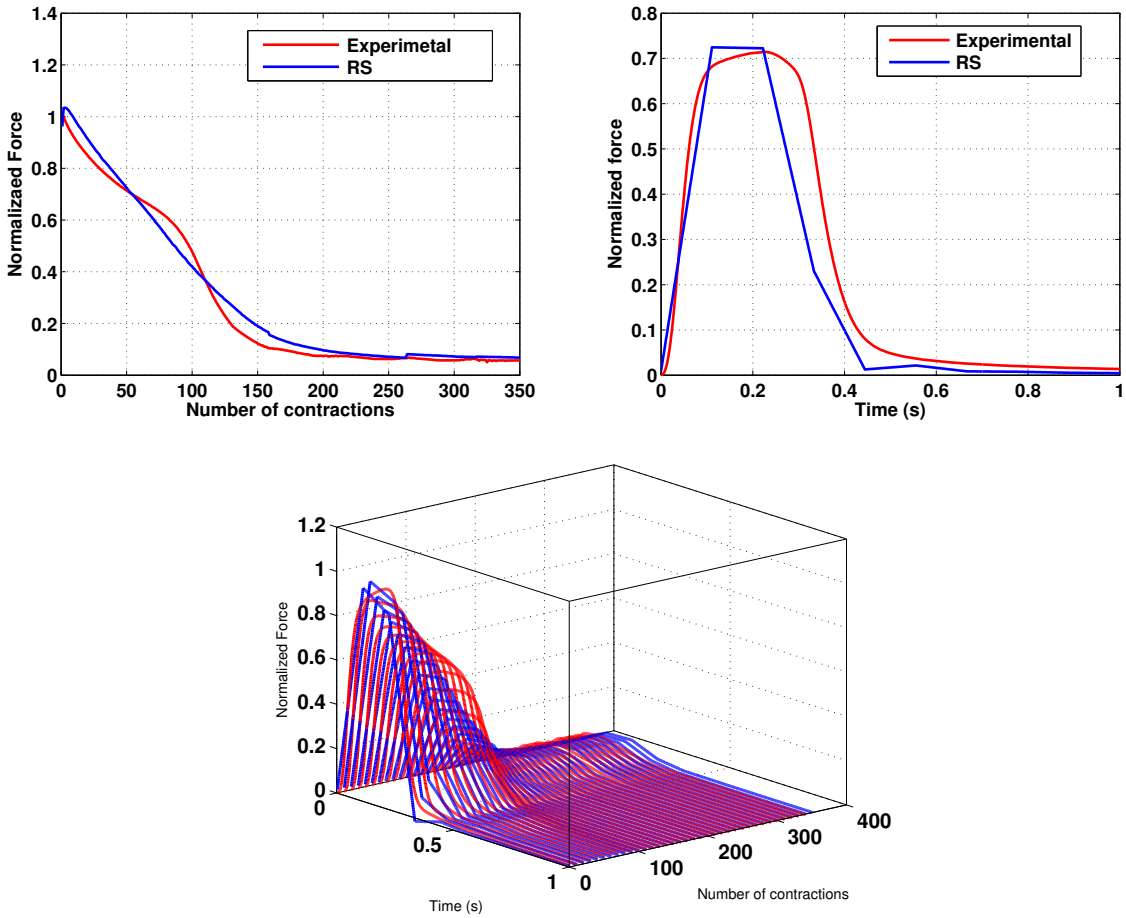

Fig. 5 a) Evolution of maximum peak force obtained by the RS (blue) and the experimental result (red). b) 50-th contraction obtained by the RS (blue) and experimentally (red). c) Contraction evolution in a 3D representation obtained by the RS (blue) and experimentally (red).

before in mammals muscles with fast fiber composition (Vedsted et al, 2003; Cairns et al, 2004, 2007; Katz et al, 2014) which agree with fast behavior described in literature (Schiaffino and Reggiani, 2011). Estimation of cross sectional area allowed us to obtain de maximum isometric stress produced by the EDL muscles. As observed in Fig. 3, our results showed a range of tensions from around 0.4 MPa to 0.6 MPa. In general, muscle tension in literature reached until 0.4 MPa in mammals. Sperringer and Grange (2016) and Head et al (2011) showed values around 0.4 MPa in mice whole muscles and the same is reported by Goodman et al (2009) in rat EDLs. The maximum tension reached by our samples (0.6 MPa) seemed to be outside of the normal range reported by other authors. Since estimation of cross sectional area in whole muscles is less accurate than in muscle fibers, it could be possible that some of these values were overestimated.

Skeletal muscle fatigue manifests as a result of repetitive or sustained muscle contraction and can be defined as a temporary reduction in the capacity of the tissue to generate force. Many protocols have been described in literature (Allen, 2004; Brotto et al, 2004; Chan and Head, 2010; Mutchler et al, 2015), however, there are several issues in both, animal and human, studies. For human, *in vivo* behavior study of an isolated muscle is complicated (Barbieri et al, 2014) and *in vitro* experiments require biopsies which are not always easy to obtain (Alghannam et al, 2014; Zampieri et al, 2015). The animal studies allow to increase the amount of samples or carry out *in vitro* experiments in a whole muscle (Bottinelli et al, 1991; Chan et al, 2008; Grasa et al, 2014). Nevertheless, a long-standing scientific challenge is to reduce the number of animals in experiments and replace them with reliable methods in order to obtain the same information. Computational models have been developed to predict the evolution of the force and to simulate the onset of fatigue. However, many of them only can fit the biological data obtained from the biological experiments (Tang et al, 2007; Böl et al, 2011; Grasa et al, 2014). The response surface presented here incorporates an important advantage in comparison with previous approximations because it allows to obtain new fatigue data from parameters not tested in animals. Furthermore, the mechanisms underlying muscle fatigue are not well understood yet. Due to the complexity of the phenomenon and the high number of factors included, the explanation has to take into account both, the molecular actin-myosin interaction and the macroscopic phenomena observed in striated muscle as well as how conditions imposed on macroscopic scales affect actin-myosin kinetics (Minozzo et al, 2012; Röhrle et al, 2012). This response surface approximation could predict not only the force obtained in a wide range of stimulation parameters but also how muscle performance change and decline inside each stimulation, because the high precision of the acquisition system allows to register the evolution of each contraction. The results provided by this technique, when focusing on the evolution of maximum peak force, are in agreement with those obtained by other authors in muscles of different specimens (Burke et al, 1973; Darques et al, 2003; Cairns et al, 2008). Regarding the human research, this information about performance is very important in the sport field, where muscle efficiency is always the most important target (Dickerson et al, 2015; Mohr et al, 2016). Moreover, one of the main advantages of the *in vitro* tests developed in this work is that the central fatigue is completely eliminated (Allen et al, 2008). This could be useful when the influence of substances in the muscle performance is investigated.

The RSPGD methodology used in this work to compute the large number of parameters considered has demonstrated that few experimental data were enough to generate the approximation and to obtain reasonable good results. The use of RSPGD do not have previous constrains for the approximation, which is not the case for traditional fitting techniques where it is useful to prescribe the approximation function type to use. This characteristic gives the technique higher flexibility to fit functions with high variations. Nevertheless, the discretization must have sufficient information in each element to obtain good response, due to the local character of the technique. The principal advantage of the methodology proposed appears in high dimensionality problems where the classical fitting procedures can not be applied (El Halabi et al, 2013b).

The results obtained could be improved in several ways, one of them involves adding more enrichment basis functions to the approximation, or adding new experimental data to enrich the sample. Another way is to change the size of the discretization for each factor. A study to optimize this discretization can be carried out, where each factor influence over the response is obtained through a previous Taguchi's design of experiments. If some factors show high variability, a better discretization for these factors must be considered, whereas, if a factor shows a constant behavior with very few elements will be enough.

Finally, mathematical models could lead into a better understanding of muscle fatigue to unveil the complex physiological phenomenon during continued muscle stimulation. Progress in this field, with the help of the technique proposed, would improve functional electrical stimulation (FES) techniques where muscle

fatigue is currently a major drawback (Shorten et al, 2007).

Acknowledgements

This work has been partially financed by Universidad de Zaragoza (Spain) under the Young Researchers'14 program (project JIUZ-2013-TEC-09), by the Spanish Ministry of Economy and Competitiveness (grant DPI 2014-54981-R) and the Department of Industry and Innovation (Government of Aragon) through the research group Grant T88 (Fondo Social Europeo) and the Instituto de Salud Carlos III (ISCIII) through the CIBER initiative.
The authors also want to thank the Tissue Characterization Platform of CIBER-BBN for technical support during the experimental tests. CIBER-BBN is an initiative funded by the VI National R&D&i Plan 2008-2011, Iniciativa Ingenio 2010, Consolider Program, CIBER Actions and financed by the Instituto de Salud Carlos III with assistance from the European Regional Development Fund.
The work was performed by the ICTS "NANBIOSIS" specifically by the Tissue & Scaffold Characterization Unit (U13), of the CIBER in Bioengineering, Biomaterials & Nanomedicne at the University of Zaragoza.

Compliance with ethical standards

Conflict of interest

No conflict of interest, financial or otherwise, are declared by the authors.

References

Alghannam AF, Tsintzas K, Thompson D, Bilzon J, Betts JA (2014) Exploring mechanisms of fatigue during repeated exercise and the dose dependent effects of carbohydrate and protein ingestion: study protocol for a randomised controlled trial. Trials 15:95

Allen DG (2004) Skeletal muscle function: role of ionic changes in fatigue, damage and disease. Clin Exp Pharmacol Physiol 31(8):485–493

Allen DG, Lamb GD, Westerblad H (2008) Skeletal muscle fatigue: cellular mechanisms. Physiol Rev 88(1):287–332

Ammar A, Mokdad B, Chinesta F, Keunings R (2006) A new family of solvers for some, classes of multidimensional partial differential equations encountered in kinetic theory modeling of complex fluids. J Non-Newton Fluid 139(3):153–176

Ammar A, Mokdad B, Chinesta F, Keunings R (2007) A new family of solvers for some classes of multidimensional partial differential equations encountered in kinetic theory modelling of complex fluids: Part ii: Transient simulation using space-time separated representations. J Non-Newton Fluid 144(2-3):98–121

Arellano-Garcia H, Schoneberger J, Korkel S (2007) Optimal design of experiments in the chemical engineering. Chem Ing Tech 79(10):1625–1638

Aslesen R, Engebretsen EM, Franch J, Jensen J (2001) Glucose uptake and metabolic stress in rat muscles stimulated electrically with different protocols. J Appl Physiol (1985) 91(3):1237–1244

Barbieri FA, Gobbi LTB, Lee YJ, Pijnappels M, van Dien JH (2014) Effect of triceps surae and quadriceps muscle fatigue on the mechanics of landing in stepping down in ongoing gait. Ergonomics 57(6):934–942

Böl M, Stark H, Schilling N (2011) On a phenomenological model for fatigue effects in skeletal muscles. J Theor Biol 281(1):122–132

Bottinelli R, Schiaffino S, Reggiani C (1991) Force-velocity relations and myosin heavy chain isoform compositions of skinned fibres from rat skeletal muscle. J Physiol 437:655–672

Brotto MAP, Nagaraj RY, Brotto LS, Takeshima H, Ma JJ, Nosek TM (2004) Defective maintenance of intracellular ca2+ homeostasis is linked to increased muscle fatigability in the mg29 null mice. Cell Res 14(5):373–378

Bruton JD, Szentesi P, Lännergren J, Westerblad H, Kovács L, Csernoch L (2000) Frog skeletal muscle fibers recovering from fatigue have reduced charge movement. J Muscle Res Cell Motil 21(7):621–628

Burke RE, Levine DN, Tsairis P, Zajac FE 3rd (1973) Physiological types and histochemical profiles in motor units of the cat gastrocnemius. J Physiol 234(3):723–48

Cairns SP, Ruzhynsky V, Renaud JM (2004) Protective role of extracellular chloride in fatigue of isolated mammalian skeletal muscle. Am J Physiol Cell Physiol 287(3):C762–C770

Cairns SP, Chin ER, Renaud JM (2007) Stimulation pulse characteristics and electrode configuration determine site of excitation in isolated mammalian skeletal muscle: implications for fatigue. J Appl Physiol (1985) 103(1):359–368

Cairns SP, Robinson DM, Loiselle DS (2008) Double-sigmoid model for fitting fatigue profiles in mouse fast- and slow-twitch muscle. Exp Physiol 93(7):851–862

Calvo B, Ramírez A, Alonso A, Grasa J, Soteras F, Osta R, Muñoz MJ (2010) Passive nonlinear elastic behaviour of skeletal muscle: experimental results and model formulation. J Biomech 43(2):318–325

Chan S, Head SI (2010) Age- and gender-related changes in contractile properties of non-atrophied edl muscle. PLoS One 5(8):e12,345

Chan S, Seto JT, MacArthur DG, Yang N, North KN, Head SI (2008) A gene for speed: contractile properties of isolated whole edl muscle from an alpha-actinin-3 knockout mouse. Am J Physiol Cell Physiol 295(4):C897–C904

Chinesta F, Ammar A, Cueto E (2010a) Proper generalized decomposition of multiscale models. Int J Numer Meth Eng 83(8-9):1114–1132

Chinesta F, Ammar A, Cueto E (2010b) Recent advances and new challenges in the use of the proper generalized decomposition for solving multidimensional models. Arch Comput Method Eng 17(4):327–350

Chinesta F, Leygue A, Bordeu F, Aguado JV, Cueto E, Gonzalez D, Alfaro I, Ammar A, Huerta A (2013) Pgd-based computational vademecum for efficient design, optimization and control. Arch Comput Method Eng 20(1):31–59

Clausen T (2013a) Excitation-induced exchange of na+, k+, and cl- in rat edl muscle in vitro and in vivo: physiology and pathophysiology. J Gen Physiol 141(2):179–192

Clausen T (2013b) Quantification of na+,k+ pumps and their transport rate in skeletal muscle: functional significance. J Gen Physiol 142(4):327–345

Clausen T, Nielsen OB (2007) Potassium, na+,k+-pumps and fatigue in rat muscle. J Physiol 584(Pt 1):295–304

Darques JL, Bendahan D, Roussel M, Giannesini B, Tagliarini F, Le Fur Y, Cozzone PJ, Jammes Y (2003) Combined in situ analysis of metabolic and myoelectrical changes associated with electrically induced fatigue. J Appl Physiol (1985) 95(4):1476–1484

de Paula Brotto M, van Leyen SA, Brotto LS, Jin JP, Nosek CM, Nosek TM (2001) Hypoxia/fatigue-induced degradation of troponin i and troponin c: new insights into physiologic muscle fatigue. Pflugers Arch 442(5):738–744

Dickerson CR, Meszaros KA, Cudlip AC, Chopp-Hurley JN, Langenderfer JE (2015) The influence of cycle time on shoulder fatigue responses for a fixed total overhead workload. J Biomech 48(11):2911–2918

Doostan A, Iaccarino G (2009) A least-squares approximation of partial differential equations with high-dimensional random inputs. J Comput Phys 228(12):4332–4345

Eberle S, Göttlinger M, Augat P (2013) Individual density-elasticity relationships improve accuracy of subject-specific finite element models of human femurs. J Biomech 46(13):2152–7

El Halabi F, Gonzalez D, Chico A, Doblare M (2013a) Fe2 multiscale in linear elasticity based on parametrized microscale models using proper generalized decomposition. Comput Meth Appl Mech Eng 257:183–202

El Halabi F, Gonzalez D, Chico-Roca A, Doblare M (2013b) Multiparametric response surface construction by means of proper generalized decomposition: An extension of the parafac procedure. Comput Meth Appl Mech Eng 253:543–557

El-Khoury R, Bradford A, O'Halloran KD (2012) Chronic hypobaric hypoxia increases isolated rat fast-twitch and slow-twitch limb muscle force and fatigue. Physiol Res 61(2):195–201

Gonzalez D, Ammar A, Chinesta F, Cueto E (2010) Recent advances on the use of separated representations. Int J Numer Methods Eng 81(5):637–659

Gonzalez D, Cueto E, Chinesta F (2014) Real-time direct integration of reduced solid dynamics equations. Int J Numer Methods Eng 99(9):633–653

Goodman CA, Horvath D, Stathis C, Mori T, Croft K, Murphy RM, Hayes A (2009) Taurine supplementation increases skeletal muscle force production and protects muscle function during and after high-frequency in vitro stimulation. J Appl Physiol (1985) 107(1):144–154

Grasa J, Sierra M, Muñoz MJ, Soteras F, Osta R, Calvo B, Miana-Mena FJ (2014) On simulating sustained isometric muscle fatigue: a phenomenological model considering different fiber metabolisms. Biomech Model Mechanobiol 13(6):1373–1385

Head SI, Greenaway B, Chan S (2011) Incubating isolated mouse edl muscles with creatine improves force production and twitch kinetics in fatigue due to reduction in ionic strength. PLoS One 6(8):e22,742

Katz A, Hernandez A, Caballero DMR, Briceno JFB, Amezquita LVR, Kosterina N, Bruton JD, Westerblad H (2014) Effects of n-acetylcysteine on isolated mouse skeletal muscle: contractile properties, temperature dependence, and metabolism. Pflugers Arch 466(3):577–585

Koutsourelakis PS (2008) Design of complex systems in the presence of large uncertainties: A statistical approach. Comput Method Appl M 197(49-50):4092–4103

Ladeveze P, Chamoin L (2011) On the verification of model reduction methods based on the proper generalized decomposition. Comput Method Appl M 200(23-24):2032–2047

Langley P, Simon HA (1995) Applications of machine learning and rule induction. Commun Acm 38(11):55–64

Lesh FH (1959) Multi-dimensional least-squares polynomial curve fitting. Commun Acm 2(9):29–30

Leygue A, Verron E (2010) A first step towards the use of proper general decomposition method for structural optimization. Arch Comput Method E 17(4):465–472

Lin YC, Farr J, Carter K, Fregly BJ (2006) Response surface optimization for joint contact model evaluation. J Appl Biomech 22(2):120–130

Minozzo FC, Hilbert L, Rassier DE (2012) Pre-power-stroke cross-bridges contribute to force transients during imposed shortening in isolated muscle fibers. PLoS One 7(1):e29,356

Mohr M, Thomassen M, Girard O, Racinais S, Nybo L (2016) Muscle variables of importance for physiological performance in competitive football. Eur J Appl Physiol 116(2):251–262

Mutchler JA, Weinhandl JT, Hoch MC, Van Lunen BL (2015) Reliability and fatigue characteristics of a standing hip isometric endurance protocol. J Electromyogr Kinesiol 25(4):667–674

Nakashima M (1995) Variable coefficient a-stable explicit runge-kutta methods. Jpn J Ind Appl Math 12(2):285–308

Neron D, Ladeveze P (2010) Proper generalized decomposition for multiscale and multiphysics problems. Arch of Comput Method E 17(4):351–372

Nirmalanandhan VS, Shearn JT, Juncosa-Melvin N, Rao M, Gooch C, Jain A, Bradica G, Butler DL (2008) Improving linear stiffness of the cell-seeded collagen sponge constructs by varying the components of the mechanical stimulus. Tissue Eng Part A 14(11):1883–91

Niroomandi S, Alfaro I, Gonzalez D, Cueto E, Chinesta F (2013a) Model order reduction in hyperelasticity: a proper generalized decomposition approach. Int J Numer Methods Eng 96(3):129–149

Niroomandi S, Gonzalez D, Alfaro I, Bordeu F, Leygue A, Cueto E, Chinesta F (2013b) Real-time simulation of biological soft tissues: a pgd approach. Int J Numer Meth Biomed 29(5):586–600

Nouy A (2007) A generalized spectral decomposition technique to solve a class of linear stochastic partial differential equations. Comput Meth Appl Mech Eng 196(45-48):4521–4537

Nouy A (2009) Recent developments in spectral stochastic methods for the numerical solution of stochastic partial differential equations. Arch of Comput Method E 16(3):251–285

Nouy A (2010) A priori model reduction through proper generalized decomposition for solving time-dependent partial differential equations. Comput Method Appl M 199(23-24):1603–1626

Nouy A, Le Maitre OP (2009) Generalized spectral decomposition for stochastic nonlinear problems. J Comput Phys 228(1):202–235

Nouy A, Clement A, Schoefs F, Moes N (2008) An extended stochastic finite element method for solving stochastic partial differential equations on random domains. Comput Method Appl M 197(51-52):4663–4682

Park HJ, Park SH (2010) Extension of central composite design for second-order response surface model building. Commun Stat-Theor M 39(7):1202–1211

Park KH, Brotto L, Lehoang O, Brotto M, Ma J, Zhao X (2012) Ex vivo assessment of contractility, fatigability and alternans in isolated skeletal muscles. J Vis Exp 1(69):e4198

Röhrle O, Davidson JB, Pullan AJ (2012) A physiologically based, multi-scale model of skeletal muscle structure and function. Front Physiol 3:358

Sakata S, Ashida F, Zako M (2007) On applying kriging-based approximate optimization to inaccurate data. Comput Methods Biomech Appl M 196(13-16):2055–2069

Schiaffino S, Reggiani C (2011) Fiber types in mammalian skeletal muscles. Physiol Rev 91(4):1447–1531

Shorten PR, O'Callaghan P, Davidson JB, Soboleva TK (2007) A mathematical model of fatigue in skeletal muscle force contraction. J Muscle Res Cell Motil 28(6):293–313

Sigal IA, Whyne CM (2010) Mesh morphing and response surface analysis: quantifying sensitivity of vertebral mechanical behavior. Ann Biomed Eng 38(1):41–56

Sperringer JE, Grange RW (2016) In vitro assays to determine skeletal muscle physiologic function. Methods Mol Biol 1460:271–291

Tang CY, Tsui CP, Stojanovic B, Kojic M (2007) Finite element modelling of skeletal muscles coupled with fatigue. Int J Mech Sci 49(10):1179 – 1191

Thornton AM, Zhao X, Weisleder N, Brotto LS, Bougoin S, Nosek TM, Reid M, Hardin B, Pan Z, Ma J, Parness J, Brotto M (2011) Store-operated ca(2+) entry (soce) contributes to normal skeletal muscle contractility in young but not in aged skeletal muscle. Aging (Albany NY) 3(6):621–634

van Lunteren E, Spiegler SE, Moyer M (2011) Fatigue-inducing stimulation resolves myotonia in a drug-induced model. BMC Physiol 11:5

Vedsted P, Larsen AH, Madsen K, Sjøgaard G (2003) Muscle performance following fatigue induced by iso-

tonic and quasi-isometric contractions of rat extensor digitorum longus and soleus muscles in vitro. Acta Physiol Scand 178(2):175–186

Wang JL, Shirazi-Adl A, Parnianpour M (2005) Search for critical loading condition of the spine–a meta analysis of a nonlinear viscoelastic finite element model. Comput Methods Biomech Biomed Engin 8(5):323–30

Zampieri S, Mosole S, Löfler S, Fruhmann H, Burggraf S, Cvečka J, Hamar D, Sedliak M, Tirptakova V, Šarabon N, Mayr W, Kern H (2015) Physical exercise in aging: Nine weeks of leg press or electrical stimulation training in 70 years old sedentary elderly people. Eur J Transl Myol 25(4):237–242

Zhao S, Li W, Gu L (2012) Biomechanical prediction of abdominal aortic aneurysm rupture risk: Sensitivity analysis. Journal of Biomedical Science and Engineering 5:664–671